Acta Cryst. (1997). A53, 810–812

Additional comments on the theoretical formulation of X-ray moiré fringes

J. YOSHIMURA *at Institute of Inorganic Synthesis, Faculty of Engineering, Yamanashi University, 4-3-11 Takeda, Kofu 400, Japan. E-mail: yoshimur@ccn.yamanashi.ac.jp*

(*Received 26 June 1997; accepted 21 July 1997*)

Abstract

Supplementary explanations are given to a theoretical formulation of X-ray moiré fringes presented in a previous paper. Properties of moiré fringes are clarified on the basis of the exact phase calculation of interfering waves. The importance of additional phase terms from the *Pendellösung* intensity oscillation and a bicrystal gap for interpreting the moiré pattern is discussed.

1. Introduction

After the early exciting studies of X-ray moiré fringes (Bonse & Hart, 1965; Chikawa, 1965; Lang & Miuscov, 1965; Simon & Authier, 1968), there have been some developments in the study in the last ten years. The nonprojectiveness of moiré-fringed diffraction images has been found by the present author (Yoshimura, 1987, 1989, 1991*a*, 1996*a*) to show that some essential details remain unknown regarding the physics of moiré fringes. The phenomenon of pseudo moiré dislocation, which is a dislocation-like fringe discontinuity in the absence of real dislocations, has been found (Yoshimura, 1996*b*). The study of interference fringes with SIMOX (separation by implanted oxygen) samples has advanced (Jiang, Simura & Rozgonyi, 1990; Prieur, Ohler & Härtwig, 1996; Ohler, Prieur & Härtwig, 1996) and it was shown that translation-fault fringes, as they were called previouly (Bonse, Hart & Schwuttke, 1969), are essentially the same as moiré fringes (Ohler, Härtwig & Prieur, 1997).

In theory, the result of a full calculation of moiré fringes by the conventional dynamical diffraction theory has been formulated in Yoshimura (1996*a*), while a satisfactory theory of moiré fringes with X-rays has not been given since the early work by Hashimoto, Mannami & Naiki (1961) for electron diffraction moiré fringes. The theory in Yoshimura (1996*a*), however, was too briefly described with the emphasis on the explanation of the theoretical projectiveness of moiré fringes and other aspects of the theory were not well explained. It is the purpose of this paper to give supplementary explanations for the main results of the theory, to advance our understanding of moiré fringes.

2. Discussion

The supplementary comments are as follows.

(i) In the theory, the moiré-producing bicrystal is assumed to be composed of parallel-sided crystals A and B having a reciprocal-lattice-vector difference $\Delta\mathbf{g}$ and a narrow gap between them. Firstly, it is clear that the effect of $\Delta\mathbf{g}$ on χ_g and χ_{-g} must be taken into account in addition to its effects on the wave vector and on the deviation parameter, since the presence of $\Delta\mathbf{g}$ means that a relative displacement $\mathbf{u}$ is produced correspondingly between the two crystals. Here, χ_g and χ_{-g} denote the Fourier components of dielecric susceptibility. Therefore, the susceptibility of the second component crystal (crystal B) should be given as follows:

$$\begin{aligned}\chi'(\mathbf{r}) &= \chi(\mathbf{r}-\mathbf{u}) \\ &= \sum_g \chi_g \exp 2\pi i[\mathbf{g}\cdot(\mathbf{r}-\mathbf{u})] \\ &= \sum_g \chi_g \exp 2\pi i\{(\mathbf{g}\cdot\mathbf{r}) + [\Delta\mathbf{g}\cdot(\mathbf{r}-\mathbf{r}_o)]\} \\ &\qquad [\because \Delta\mathbf{g} = -\mathrm{grad}(\mathbf{g}\cdot\mathbf{u})] \\ &= \sum_g [\chi_g \exp -2\pi i(\Delta\mathbf{g}\cdot\mathbf{r}_o)] \exp 2\pi i(\mathbf{g}'\cdot\mathbf{r}) \qquad (1)\end{aligned}$$

[*e.g.* see Kato's article in Azaroff *et al.* (1974)]. Here, $\mathbf{g}$ and $\mathbf{g}' = \mathbf{g} + \Delta\mathbf{g}$ are reciprocal-lattice vectors in crystals A and B, respectively; $\mathbf{r}_o$ is a position vector denoting a point for $\mathbf{u} = 0$, which is normally taken on the entrance surface b of crystal B. This origin $\mathbf{r}_o$ is not a very special point, but never an arbitrary point. The χ_g factors in crystal B are given by $\chi_{\pm g} \exp[\mp 2\pi i(\Delta\mathbf{g}\cdot\mathbf{r}_o)]$ instead of $\chi_{\pm g}$. The calculation with these χ_g factors yields the *extra* phase term $-2\pi i(\Delta\mathbf{g}\cdot\mathbf{r}_o)$ in equations (5*a*) and (5*b*) in Yoshimura (1996*a*). The equations concerned are rewritten here for the wave fields on the exit surface b' ($\mathbf{r} = \mathbf{r}_{b'}$) of crystal B:

$$I_j(\mathbf{r}_{b'}) = I_{oj}(\mathbf{r}_{b'}) + I_{gj}(\mathbf{r}_{b'}) + 2[I_{oj}(\mathbf{r}_{b'})I_{gj}(\mathbf{r}_{b'})]^{1/2} \cos\Psi_j(\mathbf{r}_{b'}) \quad (2)$$

$$\begin{aligned}\Psi_j(\mathbf{r}_{b'}) &= \varphi_{Pj}(\mathbf{r}_{b'}) + 2\pi[\Delta\mathbf{g}\cdot(\mathbf{r}_{b'}-\mathbf{r}_o)] \\ &\quad + K\alpha_{og}t_2 - (u_n t_{\mathrm{gap}}/\gamma_g) \qquad (3)\end{aligned}$$

$$K\alpha_{og} = -2\pi\{\Delta\mathbf{g}\cdot\tfrac{1}{2}[(\hat{\mathbf{K}}_o/\gamma_o) + (\hat{\mathbf{K}}_g/\gamma_g)]\} \qquad (4)$$

$$u_n = K\Delta\theta \sin 2\theta_B \qquad (5)$$

$$[j = o(\text{or } O), g(\text{or } G)].$$

Here, $I_j(\mathbf{r}_{b'})$, $I_{oj}(\mathbf{r}_{b'})$ and $I_{gj}(\mathbf{r}_{b'})$ denote the wave-field intensities in the transmitted (O beam) or diffracted beam (G beam); θ_B is the Bragg angle, K the wave number in vacuum and $\Delta\theta$ the deviation angle from the exact Bragg position at incidence on crystal A; $\hat{\mathbf{K}}_o$ and $\hat{\mathbf{K}}_g$ are unit vectors along the traveling directions of the O and G beams and $\gamma_o = (\hat{\mathbf{K}}_o\cdot\mathbf{n})$ and $\gamma_g = (\hat{\mathbf{K}}_g\cdot\mathbf{n})$, $\mathbf{n}$ being the normal vector to the crystal surfaces; t_2 is the thickness of crystal B, t_{gap} the gap width; $\varphi_{Pj}(\mathbf{r}_{b'})$ denotes a phase difference made by the extinction action or the *Pendellösung* intensity oscillation in crystals A and B and is related in a complicated way to the intensities $I_{oj}(\mathbf{r}_{b'})$ and $I_{gj}(\mathbf{r}_{b'})$.

(ii) The factor $\mathbf{l} = \frac{1}{2}[(\hat{\mathbf{K}}_o/\gamma_o) + (\hat{\mathbf{K}}_g/\gamma_g)]t_2$ in $K\alpha_{og}t_2$ geometrically gives a vector joining an incidence point and the

midpoint of the Borrmann fan on the exit surface. With this in mind, the phases having the explicit dependence on $\Delta\mathbf{g}$ in (3) can be arranged as follows:

$$\begin{aligned}\varphi_M(\mathbf{r}_{b'}) &= 2\pi[\Delta\mathbf{g}\cdot(\mathbf{r}_{b'}-\mathbf{r}_o)] + K\alpha_{og}t_2 \\ &= 2\pi[\Delta\mathbf{g}_\parallel\cdot(\mathbf{r}_{b'}-\mathbf{r}_o)_\parallel] - 2\pi(\Delta\mathbf{g}_\parallel\cdot\mathbf{l}_\parallel) \\ &= 2\pi\Delta\mathbf{g}_\parallel\cdot\{\mathbf{x}+\tfrac{1}{2}[\tan(\theta_B+\vartheta)-\tan(\theta_B-\vartheta)]\mathbf{t}\}. \quad (6)\end{aligned}$$

Here, $\mathbf{x}$ $[=(\mathbf{r}_{b'}-\mathbf{r}_o)_\parallel]$ and $\mathbf{t}$ are a coordinate and a unit vector parallel to the crystal surface, respectively, and ϑ is the angle between the diffracting plane and the surface normal. The symbol $\parallel$ denotes the parallel component to the crystal surface.

As shown, terms having the normal component of $\Delta\mathbf{g}$ to the crystal surface completely cancel in $2\pi[\Delta\mathbf{g}\cdot(\mathbf{r}_{b'}-\mathbf{r}_o)]$ and $K\alpha_{og}t_2$. According to the result in (6), the crystal moiré fringes are concerned with only the parallel component of $\Delta\mathbf{g}$ and are given as a two-dimensional scanning on the crystal surface. In the coordinate system taking the xy plane parallel to the crystal surface, $\Delta\mathbf{g}_\parallel$ is explicitly given by

$$\Delta\mathbf{g}_\parallel = [-(\Delta d/d)\cos\vartheta - \Delta\omega\sin\vartheta,\ \Delta\rho,\ 0]/d, \quad (7)$$

where d is the lattice spacing, Δd a difference in d, $\Delta\omega$ an inclination of the lattice plane about the axis $[\hat{\mathbf{K}}_o\times\hat{\mathbf{K}}_g]$ and $\Delta\rho$ a rotation about the normal to the diffracting plane. It is reconfirmed that in the symmetric geometry ($\vartheta=0$) the moiré pattern is concerned with only $\Delta d/d$ and $\Delta\rho$. In the asymmetric diffraction, $\Delta\omega$ in addition to $\Delta d/d$ and $\Delta\rho$ takes part in the formation of the moiré pattern; the fringe position shift $2\pi(\Delta\mathbf{g}_\parallel\cdot\mathbf{l}_\parallel)$ is another effect of the asymmetric diffraction. We here are confronted with an ambiguity or a question about on which surface b or b' the scanning with $\Delta\mathbf{g}_\parallel$ is made. In the theory, $\Delta\mathbf{g}$ is assumed to be constant in the bicrystal. An answer to this question can be found in Lang's (1968) experiment on the appearance and disappearance of moiré dislocations, which shows that crystal B on the inner surface b is compared with crystal A. Accordingly, $(\mathbf{r}_{b'}-\mathbf{r}_o)_\parallel$ and $\mathbf{l}_\parallel$ in (6) should be understood to be paths on the surface b.

(iii) Generally, experimental X-ray moiré fringe patterns can fully be explained when the contribution from the extinction phase $\varphi_{Pj}(\mathbf{r})$ is taken into account, as in (3). $\varphi_{Pj}(\mathbf{r})$ depends not only on the crystal thickness but on the off-Bragg deviation parameters in crystals A and B and therefore is sensitive to strain. The magnitudes of $|\varphi_{Pj}(\mathbf{r})|$ and $|\mathrm{grad}\,\varphi_{Pj}(\mathbf{r})|$ are not negligible compared to those of $|\varphi_M(\mathbf{r})|$ and $|\mathrm{grad}\,\varphi_M(\mathbf{r})|$. The difference between the fringe patterns of the O and G beams can be ascribed solely to that between $\varphi_{PO}(\mathbf{r})$ and $\varphi_{PG}(\mathbf{r})$ according to (3). Evidence of the effect of $\varphi_{Pj}(\mathbf{r})$ is commonly observed in plane-wave moiré topographs with the fringe spacing, say, of more than submillimeter order. As shown in the example in Fig. 1, local moiré patterns are different for the O and G images although the globally viewed fringe direction and spacing are practically the same; the local fringe directions are rather different between the two images and the fringe positions are displaced, typically by half the spacing. As evidenced by such disagreement between the O and G images, the observed local bendings of moiré fringes would not be a direct response to varying $\Delta\mathbf{g}$ but are produced by $\varphi_{Pj}(\mathbf{r})$, which varies locally in response to a much more minute strain. It is easily foreseen that the occurrence of pseudo moiré dislocations [as noted by the arrow in Fig. 1(a)] also is related to such locally varying $\varphi_{Pj}(\mathbf{r})$.

(iv) The gap phase $\varphi_{\mathrm{gap}} = -u_n t_{\mathrm{gap}}/\gamma_g$ is not very sensitive to the gap width change in the case that $|\Delta\theta| < 1''$ but is very sensitive to $\Delta\theta$ when $t_{\mathrm{gap}} > 100$ μm. In the case of Si (220) and Mo $K\alpha$, for example, the dependence becomes $\delta\varphi_{\mathrm{gap}}/2\pi = [\Delta\theta\delta t_{\mathrm{gap}} + t_{\mathrm{gap}}\delta(\Delta\theta)]/40$, $\Delta\theta$ and t_{gap} being given in arcsec and μm, respectively. It should be noted that the operation of φ_{gap} is not yet experimetally verified when $\Delta\mathbf{g}\neq 0$, although it is verified for the case of $\Delta\mathbf{g}=0$ (Yoshimura, 1991b).

To conclude, properties of X-ray moiré fringes have been clarified on the basis of the theoretical calculation according to the conventional dynamical diffraction theory. The reality of

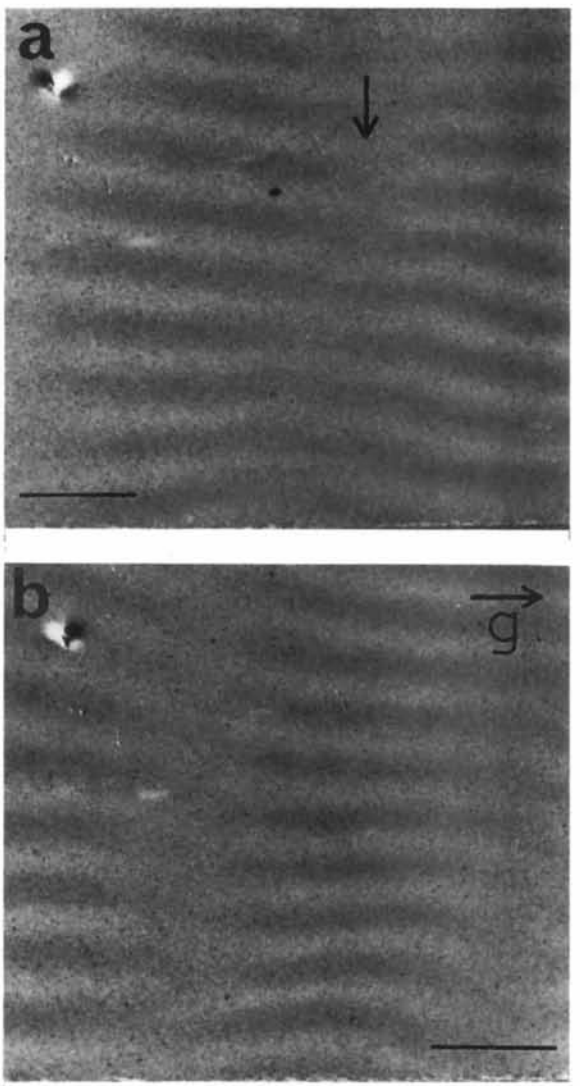

Fig. 1. A pair of plane-wave moiré topographs of a bicrystal sample. (a) O-beam image; (b) G-beam image. Taken by the synchrotron experimental set-up described by Yoshimura (1996a); Si 220 reflection, $\lambda = 0.72$ Å. The same field is shown in the two images. Dark contrast indicates stronger intensity in this case. The scale marks indicate 1 mm. Fringes viewed globally are arranged nearly parallel to the diffraction vector $\mathbf{g}$ (inclined 0–10° more precisely) with a spacing 0.43–0.55 mm. The moiré pattern is mostly due to relative rotation ($\Delta\rho = 3.5$–4.5×10^{-7} rad) between the two crystals compared. The arrow in (a) marks a pseudo moiré dislocation.

moiré fringes should further be verified by experiment. The discussion on the effect of $\varphi_{PO}(\mathbf{r})$ and $\varphi_{PG}(\mathbf{r})$ should be made more quantitatively and comprehensively. The effect of the gap width on the fringe visibility in connection with the limited coherence length of X-rays is not treated in the present calculation.

References

Azaroff, L. V., Kaplow, R., Kato, N., Weiss, R. J., Wilson, A. J. C. & Young, R. A. (1974). *X-ray Diffraction*, pp. 176–438. New York: McGraw-Hill.

Bonse, U. & Hart. M. (1965). *Appl. Phys. Lett.* **6**, 155–156.

Bonse, U., Hart, M. & Schwuttke, G. H. (1969). *Phys. Status Solidi*, **33**, 361–374.

Chikawa, J. (1965). *Appl. Phys. Lett.* **7**, 193–195.

Hashimoto, H., Mannami, M. & Naiki, T. (1961). *Philos. Trans. R. Soc. London Ser. A*, **253**, 490–516.

Jiang, B. L., Shimura, F. & Rozgonyi, G. A. (1990). *Appl. Phys. Lett.* **56**, 352–354.

Lang, A. R. (1968). *Nature (London)*, **220**, 652–657.

Lang, A. R. & Miuscov, V. F. (1965). *Appl. Phys. Lett.* **7**, 214–216.

Ohler, M., Härtwig, J. & Prieur, E. (1997). *Acta Cryst.* A**53**, 199–201.

Ohler, M., Prieur, E. & Härtwig, J. (1996). *J. Appl. Cryst.* **29**, 568–573.

Prieur, E., Ohler, M. & Härtwig, J. (1996). *Phys. Status Solidi A*, **158**, 19–34.

Simon, D. & Authier, A. (1968). *Acta Cryst.* A**24**, 527–534.

Yoshimura, J. (1987). *Acta Cryst.* A**43**, C221.

Yoshimura, J. (1989). *J. Phys. Soc. Jpn*, **58**, 1283–1295.

Yoshimura, J. (1991*a*). *Acta Cryst.* A**47**, 139–142.

Yoshimura, J. (1991*b*). *Phys. Status Solidi A*, **125**, 429–440.

Yoshimura, J. (1996*a*). *Acta Cryst.* A**52**, 312–325.

Yoshimura, J. (1996*b*). *J. Appl. Phys.* **80**, 2138–2141.